Large Scale Nanoparticle Screening for Small Molecule Analysis in Laser Desorption Ionization Mass Spectrometry

Gargey B. Yagnik,^{†,‡} Rebecca L. Hansen,^{†,‡} Andrew R. Korte,^{†,‡} Malinda D. Reichert, [†] Javier Vela, ^{†,‡} and Young Jin Lee*,^{†,‡}

Supporting Information Placeholder

ABSTRACT: Nanoparticles (NPs) have been suggested as efficient matrices for small molecule profiling and imaging by laser-desorption ionization mass spectrometry (LDI-MS), but so far there has been no systematic study comparing different NPs in the analysis of various classes of small molecules. Here, we present a large scale screening of thirteen NPs for the analysis of two dozen small metabolite molecules. Many NPs showed much higher LDI efficiency than organic matrices in positive mode and some NPs showed comparable efficiencies for selected analytes in negative mode. Our results suggest that a thermally driven desorption process is a key factor for metal oxide NPs, but chemical interactions are also very important, especially for other NPs. The screening results provide a useful guideline for the selection of NPs in the LDI-MS analysis of small molecules.

The use of nanoparticles (NPs) as a matrix for laser-desorption ionization mass spectrometry (LDI-MS) goes back to Nobel laureate Koichi Tanaka's initial work using 30 nm size cobalt powder to desorb and ionize proteins in 1988. Nanoparticles have many advantages as LDI matrices, including vacuum stability, good laser absorption, homogeneous application (no "sweet spots"), and almost no matrix background in the low-mass region. In addition, their high surface areas can be used for the enrichment of certain classes of compounds, enabling high-throughput selective analysis.

In spite of these advantages, NPs have been neglected because organic matrices have been found to be more efficient for LDI-MS of biological macromolecules. Nanoparticles gained renewed attention with the success of nanostructure-based surface ionization, such as desorp-

tion/ionization on silicon (DIOS)³ and nanostructure-initiator mass spectrometry (NIMS)⁴. Encouraged by this success and the advancement of various nanoparticle synthesis⁵, the use of NPs for LDI-MS, termed nanoparticle-assisted LDI-MS or NALDI-MS, has flourished in recent years^{2,6}. Gold and silver NPs have been most widely adopted, thanks to the availability of various synthetic routes⁶⁻⁹, but the field has recently expanded into a wider range of NPs, including metal oxide NPs (e.g., TiO₂¹⁰, Fe₃O₄¹¹, ZnO¹²), carbon-based NPs (e.g., colloidal graphite¹³, graphene oxide¹⁴, nanodiamond¹⁵), metal NPs (e.g., platinum¹⁶, copper¹⁷), and semi-conductor quantum dots (e.g., CdSe¹⁸, ZnS¹⁹, HgTe²⁰). Most of these studies, however, were performed for one or two limited classes of compounds, mostly peptides, proteins, oligosaccharides, or polyethylene glycols (PEG), and application to small molecules has been very limited. This is counterintuitive because one of the most important benefits of NPs as matrices is the lack of background in the low mass region.

Most NALDI-MS studies use capping materials to improve stability; these capping materials can provide additional benefits such as enrichment of specific target compounds, ^{2,21,22} enhancement of ionization efficiency, ^{23,24} and evaluation of biocompatibility for drug delivery. ^{25,26} This is especially important for metal NPs because they are prone to aggregate without capping. ²⁶ While this approach has been well demonstrated for proteins ²⁷ or other macromolecules, ²⁸ its application to small molecules is relatively rare. ^{29,30} In fact, organic capping compounds are easily released during NALDI-MS, and cause significant interferences and ion suppression in small molecule analysis. ²⁹ Capping is thus typically undesirable for small molecule applications. Nanoparticles without capping, however, often exhibit analyte selectivity and it is generally not well established which non-functionalized NPs enhance which classes of

 $^{^\}dagger$ Department of Chemistry, Iowa State University, Ames, IA 50011, USA

[‡]Ames Laboratory-US DOE, Ames, IA 50011, USA

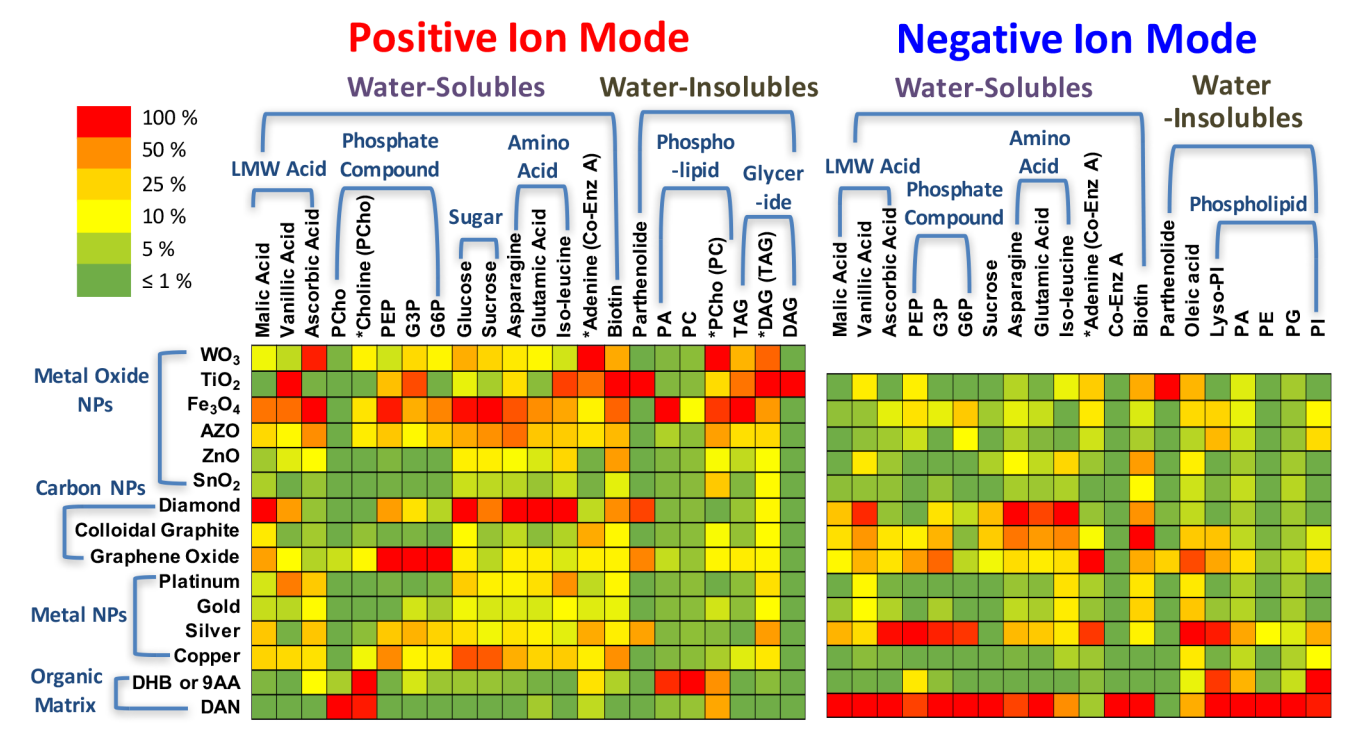


Figure 1. Summary of nanoparticle screening for small molecule metabolite analysis. Ion signals are normalized to the highest ion signal for each analyte and shown as a heat map. WO3 NPs have significant matrix background in negative mode and were not used for the final screening. An asterisk indicates a fragment ion with the precursor shown in parenthesis. Acronyms used for analytes are listed in Suppl. Info. DHB: 2,5-dihydroxybenzoic acid, 9AA: 9-aminoacridine, DAN: 1,5-diaminonaphthalene. DHB and DAN were used for positive ion mode and 9AA and DAN were used for negative ion mode.

small molecules. Some NPs are known for their efficiency in the analysis of specific compounds (e.g., Ag for olefins, Ag and Au for sulfur compounds), but the behavior of other NPs is mostly unknown.

Here, we report a large-scale study of the suitability of several NP types for NALDI-MS of small molecule metabolites. The nanoparticles used in this study include metal oxide NPs (WO₃, TiO₂, Fe₃O₄, AZO [aluminum-doped zinc oxide], ZnO, SnO₂), carbon-based NPs (boron doped nanodiamond, colloidal graphite, graphene oxide), and metal NPs (Pt, Au, Ag, Cu). All of these NPs are not functionalized, except for some carbon-based NPs, which are inherently functionalized during synthesis. The small molecule metabolites used in this study were combined into two groups, water-soluble and water-insoluble (Figure S1), for the convenience of sample preparation and analyzed separately. Figure 1 summarizes our NP screening as a heat map (raw data are in Tables S1 and S2), as compared to two widely employed organic matrices in positive and negative ion modes, under optimized conditions for each NP or matrix (see Suppl. Info for details). In positive ion mode, NPs show minimal matrix peaks (Figure S2) and outperform organic matrices except in the cases of phosphocholine (PCho), phosphatidylcholine (PC), and phosphatidic acid (PA). In negative ion mode, the organic matrix DAN, recently reported as a useful matrix for small molecule and lipid analysis in negative mode^{31,32}, is superior to almost all NPs; however, some NPs show comparable signals for selected analytes.

Many metal oxide NPs work well in positive mode, especially Fe₃O₄ and TiO₂. We have developed a thermal desorption model modified from Schurenberg et al.³³ (Suppl. Info), which explains high NALDI efficiency with metal oxide and diamond NPs. In short, metal oxide and boron-doped diamond NPs have good laser absorption, high heat capacity and low thermal conductivity, and they can be heated to a high temperature by the laser irradiation, which leads to the efficient desorption of nearby analytes. This process is thermally driven and is mostly analyte-independent, as demonstrated by the broad coverage afforded by these NPs. WO₃ NPs have the lowest heat conductivity, resulting in the highest temperature by laser irradiation ($T_{cal} = 2,446$ K; Table S5) in agreement with the significant fragmentations of PCho, co-enzyme A, PC, and triacylglycerol (TAG) (* labeled fragments in Figure 1). Fe₃O₄, TiO₂, and diamond NPs produce high temperatures (T_{cal} = 1,064, 1,246, and 1,431 K, respectively; Table S5), in concord with their high NALDI efficiency.

Some NPs show unique, analyte-dependent specificity, which is consistent in both positive and negative ion mode. Diamond NPs work well for sugars and amino acids, graphene oxide and silver NPs for phosphate compounds, and TiO₂ for parthenolide (a terpene). This cannot be explained by the thermal desorption model

only; chemical interactions must be important either in solution before samples are spray-deposited onto the MALDI plate or in the gas phase laser plume. To test the hypothesis that the ability of some analytes to adsorb to specific NPs may lead to more efficient desorption of those analytes, an experiment was performed after incubation of the water-soluble analyte mixture with selected NPs for an hour prior to deposition onto the MALDI plate. As shown in Figure 2, Fe₃O₄ and TiO₂ NPs show a slight decrease in signal intensity for most analytes after incubation, graphene oxide NPs show minimal change, and diamond NPs show a dramatic increase for most analytes. An increase in signal is especially prominent with malic acid, vanillic acid, sugars, amino acids, and biotin, consistent with the LDI efficiency of diamond NPs in Figure 1. However, this adsorption effect cannot completely explain all the LDI efficiency (e.g., TiO₂ has the best NALDI efficiency for vanillic acid, but adsorption leads to the decrease of the ion signal), suggesting gas phase ionization or other chemical interactions must also play a role.

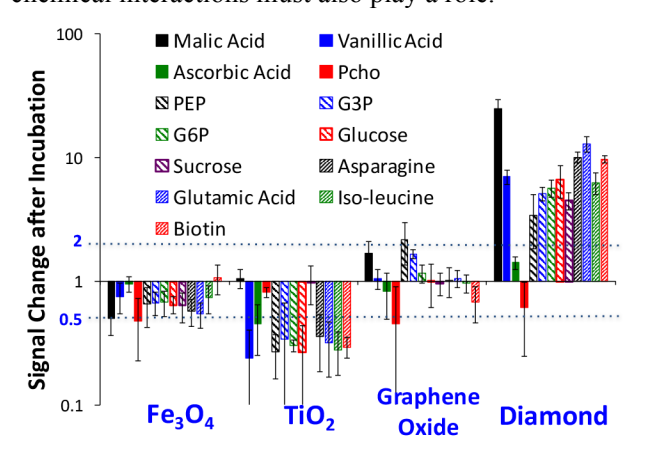


Figure 2. Signal change of water-soluble analytes after 1hr in-solution incubation prior to spray-deposition to MALDI plate, compared to immediate deposition.

Because of their broad light absorption and widespread availability, carbon-based NPs have been widely used for NALDI-MS. 13,34,35 Among the carbon-based NPs used in this study, boron-doped diamond NPs showed the best overall performance, but graphene oxide NPs showed better performance for phosphate compounds and oleic acid, while colloidal graphite NPs showed better performance for biotin in negative mode. The good performance of diamond NPs in this study is opposite to that observed by Tang et al.³⁴, where diamond NPs showed the lowest ionization efficiency for benzylpyridinium ion among various carbon-based NPs. We attribute this difference to the thousand times higher laser absorption of boron-doped diamond NPs compared to pure diamond. 36 An important attribute of diamond NPs is their high thermal stability. Unlike graphene oxide or colloidal graphite, diamond NPs produce almost no carbon cluster peaks in positive ion mode and minimal peaks in negative ion mode (Figure S6). The

high thermal stability of diamond NPs likely allows efficient desorption and ionization of analytes, instead of producing carbon clusters. Carbon-based NPs show analyte-specific LDI efficiencies, which likely arise from interactions between analytes and diverse functional groups on the NP surfaces (FTIR spectra in Figure S9).

Metal NPs have been widely utilized for various applications, 6,7,16 mostly with capping agents. Here, bare NPs were not very efficient, likely because of their tendency to aggregate without capping. Platinum NPs especially were very difficult to keep in suspension, as aggregation was visible to the naked eye within a few seconds. Gold NPs were also unstable, starting to aggregate within a few minutes. Silver and copper NPs did not show apparent aggregation within the time scale of this experiment, and do show good results for some analytes; however, SEM images show some aggregation (Figure S8). Recently, vacuum sputter deposition has been suggested as a useful method for in situ synthesis and deposition of silver NPs for NALDI-MS. 37-39 This method does not induce any aggregation, and might be also useful for other metal NPs, but was not explored in the current study.

The high NALDI efficiency of parthenolide with TiO₂ NPs, both in positive and negative mode, is intriguing considering the difficulty of terpene ionization by most other NPs or organic matrices. Recently, we were able to analyze phytocassanes and momilactones (both terpenes) with TiO2 and Fe3O4 NPs, but not with any organic matrices. 40 Fe₃O₄ NPs showed higher sensitivity for this class of terpenes than TiO2 NPs, which contrasts with parthenolide in the current study where Fe₃O₄ NPs are mostly inefficient. Further study is necessary to achieve a more detailed understanding, but we tentatively conclude that 1) high temperature is essential for terpenes because of their high boiling point compared to other analytes, as evidenced by their high efficiency with some metal oxide NPs and diamond NPs, and 2) chemical interactions also play an important role for these hydrophobic compounds that are difficult to ionize (e.g., momilactones and phytocassanes have hydroxyl groups but not parthenolide).

In conclusion, we have shown NPs are highly efficient matrices for LDI-MS of a wide range of small molecules, especially in positive mode but also in negative mode for certain compounds. A thermal desorption model partially explains NALDI efficiency, but chemical interactions are also important. We anticipate our screening result will be very useful to many researchers in the selection of NPs for NALDI-MS analysis of their small molecules of interest. For example, DHB is most commonly used for the analysis of TAG, but the ion suppression of TAG by PC is well known. According to this study, Fe₃O₄ NPs would be much more effective than DHB for the analysis of TAG even in the the presence of PC. Similarly, we expect TiO₂ NPs would be useful for DAG, biotin, and terpene. Selectivity of NPs

could be utilized for the high-throughput analysis of specific compounds in complex mixtures.

ASSOCIATED CONTENT

Supporting Information.

Experimental, supplementary tables and figures, and miscellaneous discussion.

This material is available free of charge via the Internet at http://pubs.acs.org.

AUTHOR INFORMATION

Corresponding Author

*yjlee@iastate.edu

Notes

No competing financial interests have been declared.

ACKNOWLEDGMENT

This work was supported by the U.S. Department of Energy (DOE), Office of Basic Energy Sciences, Division of Chemical Sciences, Geosciences and Biosciences. The Ames Laboratory is operated by Iowa State University under DOE Contract DE-AC02-07CH11358.

REFERENCES

- (1) Tanaka, K.; Waki, H.; Ido, Y.; Akita, S.; Yoshida, Y.; Yoshida, T.; Matsuo, T. *Rapid Commun. Mass Spectrom.* **1988**, 2, 151.
- (2) Chiang, C.-K.; Chen, W.-T.; Chang, H.-T. *Chem. Soc. Rev.* **2011**, *40*, 1269.
- (3) Thomas, J. J.; Shen, Z. X.; Blackledge, R.; Siuzdak, G. *Anal. Chim. Acta* **2001**, *442*, 183.
- (4) Northen, T. R.; Yanes, O.; Northen, M. T.; Marrinucci, D.; Uritboonthai, W.; Apon, J.; Golledge, S. L.; Nordstrom, A.; Siuzdak, G. *Nature* **2007**, *449*, 1033.
- (5) Modeshia, D. R.; Walton, R. I. Chem. Soc. Rev. 2010, 39, 4303.
- (6) Pilolli, R.; Palmisano, F.; Cioffi, N. *Anal. Bioanal. Chem.* **2012**, *402*, 601.
- (7) Sekula, J.; Niziol, J.; Rode, W.; Ruman, T. *Analyst* **2015**, *140*. 6195.
- (8) Sherrod, S. D.; Diaz, A. J.; Russell, W. K.; Cremer, P. S.; Russell, D. H. *Anal. Chem.* **2008**, *80*, 6796.
 - (9) Huang, Y. F.; Chang, H. T. Anal. Chem. 2006, 78, 1485.
- (10) Shrivas, K.; Hayasaka, T.; Sugiura, Y.; Setou, M. Anal. Chem. **2011**, 83, 7283.
- (11) Chiang, C.-K.; Chiang, N.-C.; Lin, Z.-H.; Lan, G.-Y.; Lin, Y.-W.; Chang, H.-T. *J. Am. Soc. Mass Spectrom.* **2010**, *21*, 1204.
- (12) Gedda, G.; Abdelhamid, H. N.; Khan, M. S.; Wu, H.-F. RSC Advances **2014**, *4*, 45973.
 - (13) Cha, S.; Yeung, E. S. Anal. Chem. 2007, 79, 2373.
- (14) Kim, Y.-K.; Na, H.-K.; Kwack, S.-J.; Ryoo, S.-R.; Lee, Y.; Hong, S.; Hong, S.; Jeong, Y.; Min, D.-H. *Acs Nano* **2011**, *5*, 4550
- (15) Wei, L.-M.; Xue, Y.; Zhou, X.-W.; Jin, H.; Shi, Q.; Lu, H.-J.; Yang, P.-Y. *Talanta* **2008**, *74*, 1363.
- (16) Kawasaki, H.; Yonezawa, T.; Watanabe, T.; Arakawa, R. Journal of Physical Chemistry C 2007, 111, 16278.
- (17) Yonezawa, T.; Kawasaki, H.; Tarui, A.; Watanabe, T.; Arakawa, R.; Shimada, T.; Mafune, F. *Anal. Sci.* **2009**, *25*, 339.
- (18) Shrivas, K.; Kailasa, S. K.; Wu, H.-F. *Proteomics* **2009**, 9, 2656
 - (19) Kailasa, S. K.; Wu, H.-F. Analyst 2010, 135, 1115.
- (20) Chiang, C.-K.; Yang, Z.; Lin, Y.-W.; Chen, W.-T.; Lin, H.-J.; Chang, H.-T. *Anal. Chem.* **2010**, *82*, 4543.
 - (21) Huang, Y.-F.; Chang, H.-T. Anal. Chem. 2007, 79, 4852.

- (22) Kailasa, S. K.; Wu, H.-F. *TrAC, Trends Anal. Chem.* **2015**, 65, 54.
- (23) Castellana, E. T.; Russell, D. H. *Nano Lett.* **2007**, *7*, 3023. (24) Duan, J.; Linman, M. J.; Chen, C.-Y.; Cheng, Q. J. *J. Am. Soc. Mass Spectrom.* **2009**, *20*, 1530.
- (25) Yan, B.; Kim, S. T.; Kim, C. S.; Saha, K.; Moyano, D. F.; Xing, Y.; Jiang, Y.; Roberts, A. L.; Alfonso, F. S.; Rotello, V. M.; Vachet, R. W. *J. Am. Chem. Soc.* **2013**, *135*, 12564.
- (26) Zhu, Z.-J.; Tang, R.; Yeh, Y.-C.; Miranda, O. R.; Rotello, V. M.; Vachet, R. W. *Anal. Chem.* **2012**, *84*, 4321.
- (27) Kong, X. L.; Huang, L. C. L.; Hsu, C. M.; Chen, W. H.; Han, C. C.; Chang, H. C. *Anal. Chem.* **2005**, *77*, 259.
- (28) Tang, J.; Liu, Y.; Qi, D.; Yao, G.; Deng, C.; Zhang, X. *Proteomics* **2009**, *9*, 5046.
- (29) Amendola, V.; Litti, L.; Meneghetti, M. Anal. Chem. 2013, 85, 11747.
- (30) Taira, S.; Sugiura, Y.; Moritake, S.; Shimma, S.;
- Ichiyanagi, Y.; Setou, M. Anal. Chem. 2008, 80, 4761.
- (31) Korte, A. R.; Lee, Y. J. J. Mass Spectrom. 2014, 49, 737.
- (32) Thomas, A.; Charbonneau, J. L.; Fournaise, E.; Chaurand, P. *Anal. Chem.* **2012**, *84*, 2048.
- (33) Schurenberg, M.; Dreisewerd, K.; Hillenkamp, F. Anal. Chem. 1999, 71, 221.
- (34) Tang, H.-W.; Ng, K.-M.; Lu, W.; Che, C.-M. Anal. Chem. **2009**, *81*, 4720.
- (35) Najam-ul-Haq, M.; Rainer, M.; Szabo, Z.; Vallant, R.; Huck, C. W.; Bonn, G. K. *J. Biochem. Biophys. Methods* **2007**, 70, 319
- (36) Gajewski, W.; Achatz, P.; Williams, O. A.; Haenen, K.; Bustarret, E.; Stutzmann, M.; Garrido, J. A. *Physical Review B* **2009**, 79, 045206.
- (37) Jackson, S. N.; Baldwin, K.; Muller, L.; Womack, V. M.; Schultz, J. A.; Balaban, C.; Woods, A. S. *Anal. Bioanal. Chem.* **2014**, *406*, 1377.
- (38) Lauzon, N.; Dufresne, M.; Chauhan, V.; Chaurand, P. J. Am. Soc. Mass Spectrom. **2015**, 26, 878.
- (39) Xu, L.; Kliman, M.; Forsythe, J. G.; Korade, Z.; Hmelo, A. B.; Porter, N. A.; McLean, J. A. *J. Am. Soc. Mass Spectrom.* **2015**, *26*, 924.
- (40) Klein, A. T.; Yagnik, G. B.; Hohenstein, J. D.; Ji, Z.; Zi, J.; Reichert, M. D.; MacIntosh, G. C.; Yang, B.; Peters, R. J.; Vela, J.; Lee, Y. J. Anal. Chem. **2015**, *87*, 5294.
- (41) Emerson, B.; Gidden, J.; Lay, J. O., Jr.; Durham, B. *J. Lipid Res.* **2010**, *51*, 2428.

